

Evaluating the accuracy of gridded water resources reanalysis and evapotranspiration products for assessing water security in ungauged basins

Elias Nkiaka¹, Robert G. Bryant¹, Joshua Ntajal^{2,3}, Eliezer I. Biao⁴

¹Department of Geography, University of Sheffield, Sheffield, S10 2TN, UK

²Department of Geography, University of Bonn, 53115 Bonn, Germany

³Center for Development Research, University of Bonn, 53113 Bonn, Germany

⁴Laboratory of Applied Hydrology, University of Abomey-Calavi (UAC), Cotonou, Benin

Elias Nkiaka (Corresponding author): e.nkiaka@sheffield.ac.uk

Postal Address: Department of Geography, University of Sheffield, Sheffield, S10 2TN, UK

Abstract

Achieving water security in ungauged basins is critically hindered by a lack of in situ river discharge data to assess past, current and future evolution of water resources. To overcome this challenge, there has been a shift toward the use of freely available satellite and reanalysis data products. However, due to inherent bias and uncertainty, these secondary sources require careful evaluation to ascertain their performance before being applied in ungauged basins. The objectives of this study were to evaluate river discharge and evapotranspiration estimates from eight gridded water resources reanalysis (WRR), six satellite-based evapotranspiration (ET) products and ET estimates derived from complimentary relationship (CR-ET) across eight river basins located in Central-West Africa. We also estimated the relative uncertainties in monthly basin-scale water balance evapotranspiration (ET_{WB}) across all the basins. Results highlight strengths and weaknesses of the different WRR in simulating discharge dynamics and ET across the basins. Likewise satellite-based products also show some strength and weaknesses in simulating monthly ET. Analyses further revealed that the relative uncertainties in monthly ET_{WB} range from 4–25 % with a significant increase in magnitude during the rainy season while river discharge appear to be the dominant source of uncertainty. Our results further revealed that the performance of the models in simulating river discharge and evapotranspiration is strongly influenced by model structure, input data and spatial resolution. Considering all the evaluation criteria Noah, Lisflood, AWRAL, and Terra are among the best performing WRR products while Noah, Terra, GLEAM3.5a & 3.5b, and PMLV2 produced ET estimates with the least bias. Considering the plethora of products available, it is imperative to evaluate their performance in representative gauged basins to identify products that can be applied in each region. However, the choice of a particular WRR or ET product will depend on the application and users requirements. Results from this study suggest that gridded WRR and ET products are a useful source of data for assessing water security in ungauged basins.

34 **1. Introduction**

35 River discharge is one of the most important hydrological variables underpinning water resources
36 management, aquatic ecosystems sustainability, flood prediction, and drought warnings at different
37 scales (McNally et al., 2017; Couasnon et al., 2020). However, observed river discharge data is often
38 not available at the exact location where critical water management decisions need to be made (Neal
39 et al., 2009). This is especially the case in developing and semi arid/arid regions where discharge
40 gauging stations are sparse (Krabbenhof et al., 2022), while the number of existing stations are
41 declining (Rodríguez et al., 2020). Despite the acute shortage in observed data, developing regions
42 are areas that are more vulnerable to adverse hydroclimatological conditions (Byers et al., 2018;
43 Kabuya et al., 2020). Furthermore, achieving water security in ungauged basins in developing regions
44 remains a critical development challenge as climate change, population growth, rapid urbanization,
45 and economic growth continue to exert pressure on available water resources under hydrological
46 uncertainty (Flörke et al., 2018; Hirpa et al., 2019). This highlights the urgent need for more reliable
47 data to better assess past, current, and future evolution of water resources, and to predict extreme
48 hydroclimatological events so that better strategies can be put in place to enhance water management
49 and mitigate the impact of extreme events (Nkiaka et al., 2020; Slater et al., 2021). Water security in
50 this study refers to the availability of sufficient quantities of water for human use and ecosystem
51 sustainability.

52 Evapotranspiration (ET) is another important hydrological variable that represents the linkage
53 between water, energy and carbon cycles and ecosystem services and is the second largest process in
54 the hydrological cycle after precipitation (Zhang et al., 2019). Therefore, ET plays a critical role in
55 water availability at different scales. As such, accurate estimates of ET are also crucial for water
56 management operations such as basin-scale water balance estimation, irrigation planning, estimating
57 water footprint, and assessing the impact of climate change on water availability. However, globally,
58 in situ ET monitoring stations are also scarce while the existing monitoring network cannot provide
59 sufficient information on the temporal and spatial trends of ET at large scales (Laipelt et al., 2021).
60 ET data scarcity may therefore limit our ability to understand changes in the hydrological cycle and
61 water security in the context of environmental change and hydrological uncertainty.

62 To enhance water security in ungauged basins, there has been a progressive shift toward the
63 use of gridded data derived from satellite and reanalysis (Oduanya et al., 2019; Nkiaka, 2022). This
64 is because gridded data products can provide high spatial resolution and long-term homogeneous data
65 for previously unmonitored areas at scales that are suitable for studying changes in the hydrological
66 cycle and for water management applications (Sheffield et al., 2018). Several gridded data products
67 with global coverage have been produced in recent decades including reanalysis and satellite-based
68 products. Examples of reanalysis products include Watch Forcing Data applied to ERA-Interim

69 (Weedon et al., 2014) and Climate Forecast System Reanalysis (Saha et al., 2014). There is also a
70 plethora of satellite products for different hydrometeorological variables such as precipitation,
71 temperature, soil moisture, and ET. For satellite derived ET estimates, it is worth noting that this
72 variable cannot be directly measured by satellites, but rather derived from physical variables observed
73 by satellites from space such as radiation flux. As such, satellite derived ET estimates could rather be
74 referred to as model outputs constrained by satellite data. Another technique used to produce ET
75 estimates is the complimentary relationship (Ma et al., 2021). Considering the way gridded ET
76 products are derived, they tend to suffer from large biases (Weerasinghe et al., 2020; Mcnamara et
77 al., 2021) and therefore need to be validated before use. In fact, it is argued that validating gridded
78 ET products is an essential step in understanding their applicability and usefulness in water
79 management operations (Blatchford et al., 2020).

80 Previously, much attention in the development of gridded environmental data was focused on
81 hydrometeorological variables such as precipitation and temperature. However, rapid advancement
82 in computer technology has led to the development of gridded water resources reanalysis (WRR) with
83 quasi global coverage using both land surface models (LSMs) and Global Hydrological Models
84 (GHMs) driven by satellite and reanalysis data. Examples of WRR products include the Global Land
85 Data Assimilation System [GLDAS] (Rodell et al., 2004), “The Global Earth Observation for
86 Integrated Water Resources Assessment” [earth2Observe] (Schellekens et al., 2017), and the Global
87 Flood Awareness System [GloFAS-ERA5] (Harrigan et al., 2020). Several studies have demonstrated
88 that model-based gridded WRR products can be used as an alternative to observe river discharge in
89 ungauged basins to: (1) understand hydrological processes (Koukoula et al., 2020), (2) support
90 transboundary water management (Sikder et al., 2019), (3) identify flood events (Gründemann et al.,
91 2018; López et al., 2020), and (4) support national water policies (Rodríguez et al., 2020). These
92 examples demonstrate that WRR products have great potential for addressing water security
93 challenges in ungauged basins. Despite their numerous advantages, model outputs from WRR are
94 also fraught with uncertainties resulting from errors in the forcing data, model structure, and the
95 parameterisation of the physical processes in the model scheme (Koukoula et al., 2020). Therefore, it
96 is necessary to evaluate the performance of these products against observed river discharge where
97 available.

98 Whilst the use of outputs from WRR in water management has gained significant attention in
99 many ungauged or poorly gauged regions such as Asia and Latin America (López et al., 2020;
100 Rodríguez et al., 2020; Sikder et al., 2019), they remain largely under-utilized in Africa. For example,
101 there are only a few case studies reporting on the use of these products in the Upper Blue Nile River
102 basin (Koukoula et al., 2020; Lakew et al., 2020) and the Zambezi River basin (Gründemann et al.,
103 2018). Considering the scale of water insecurity in Africa -compounded by acute data scarcity

104 (Nkiaka et al., 2021), we feel that evaluating the performance of gridded WRR products in Africa
105 may enhance their adoption in water management in the region. On the other hand, several studies
106 evaluating the performance of gridded data in Africa have focused mostly on precipitation (Dinku et
107 al., 2018; Satgé et al., 2020) while few studies that have evaluated gridded ET products focused on
108 large basins, (Blatchford et al., 2020; Weerasinghe et al., 2020; Mcnamara et al., 2021) and mostly
109 adopting an annual timescale. This may be attributed to the large scale of the basins which is ideal
110 for the application of satellite data and the coarse spatial resolution of some of the ET products. The
111 availability of high spatial and temporal resolution ET products means that it is now possible to evaluate
112 these products in small- to medium-size basins and at a higher temporal resolution. Lastly,
113 considering that the water balance concept has been used widely to evaluate gridded ET products,
114 most studies did not account for uncertainties in basin-wide water balance evapotranspiration (ET_{WB})
115 even though such uncertainties could be large (Baker et al., 2021).

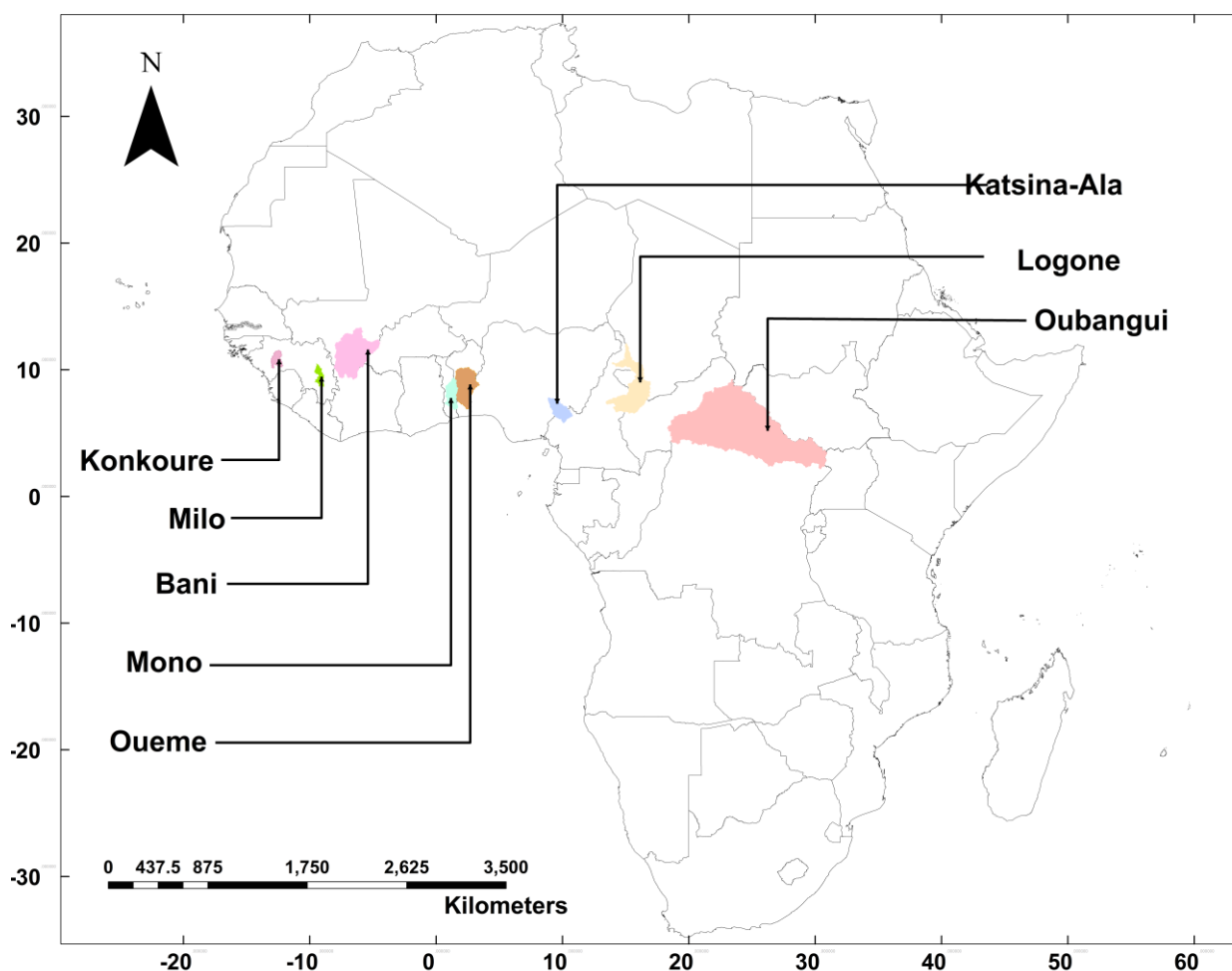
116 The objectives of this paper were to: (1) evaluate the performance of earth2Observe Tier 1
117 and other WRR products in simulating discharge and evapotranspiration in the basins, (2) evaluate
118 the performance of six satellite-based gridded ET estimates and ET estimates obtained using the
119 complementary relationship (CR-ET) and (3) estimate the relative uncertainties in ET_{WB} in the
120 basins. Considering that only a few studies have attempted to evaluate gridded WRR and ET products
121 over Africa, this paper contributes to the contemporary debate on the performance of these products
122 and how they can be used to assess water security in ungauged basins. We evaluated ET estimates
123 from WRR and other sources considering the fact that users' needs for the application of these products
124 may vary. Hence our evaluation covered a wide range of models and products that meet the needs of
125 different users.

126 **2. Materials and methods**

127 **2.1. Study area**

128 The selected basins are located in Central-West Africa ranging in size from 9,000 km² to 499,000
129 km² (Figure 1). Rainfall in the region is mostly controlled by the north-south movement of the
130 intertropical convergence zone (ITCZ). The main criteria for selecting the basins were: (1) availability
131 of observed river discharge data and (2) for the period of the available discharge data to coincide with
132 the period when gridded WRR and ET data are also available. Additionally, some of the selected
133 basins are facing substantial water security challenges caused by population displacement from
134 conflicts in the Sahel and Lake Chad regions (Kamta et al., 2021; Nagabhatla et al., 2021). The
135 evaluation timestep was determined by the timestep of river discharge data. Shapefiles for all the
136 basins were obtained from HydroSHEDS, locations of the discharge gauging stations were obtained
137 from the respective data sources while the area of each basin was calculated from the basin shapefiles.

138 HydroSHEDS drainage network offers the unique opportunity to generate watershed boundaries for
 139 GRDC gauging stations using a proofed dataset and applying a consistent methodology. Table 1
 140 shows that some of the basins are transboundary in nature.



141
 142 **Figure 1:** Locations of the eight river basins where the performance of WRR and gridded ET
 143 products were evaluated

144 **Table 1:** Characteristics of river basins and sources of river discharge data

Basin	Total area (km ²)	Transboundary (Yes or No) Countr(y/ies)	Population (thousands)	Source of river discharge data
Bani	101,600	(Yes) Ivory Coast, Mali, and Burkina Faso	63,766	GRDC
Katsina-Ala	22,963	(Yes) Cameroon and Nigeria	219,875	NHSA
Konkoure	10,250	(No) Guinea-Conakry	13,053	GRDC
Logone	87,953	(Yes) Cameroon, Chad, and Central Africa Republic	44,272	LCBC
Milo	9,620	(No) Guinea-Conakry	13,053	GRDC
Mono	21,575	(Yes) Togo, Benin	21,479	Co-author
Oubangui	499,000	(Yes) Central Africa Republic and the Democratic Republic of Congo	88,742	GRDC
Oueme	46,990	(No) Benin	11,488	Co-author

145 Global River Discharge Centre [GRDC], Nigeria Hydrological Services Agency [NIHSA], Lake Chad Basin Commission
 146 [LCBC]. Population data sourced from (Undesa, 2019)

147

148

2.2. Input data

2.2.1. Water resources reanalysis (WRR0)

The WRR product evaluated in this study include “The Global Earth Observation for Integrated Water Resources Assessment” (earth2Observe), Famine Early Warning Systems Network [FEWS NET] Land Data Assimilation System (FLDAS), and TerraClimate. The earth2Observe Tier 1 product consists of a multi-model ensemble of ten global models at a spatial resolution of $0.5^\circ \times 0.5^\circ$ spanning from 1979 to 2012 and driven by Watch Forcing Data methodology applied to ERA-Interim reanalysis (WFDEI) data (Schellekens et al., 2017). The WRR from earth2Observe project are freely available through the project data portal (<https://wci.earth2observe.eu/portal/>). Model evaluation here omits the Joint UK Land Environment Simulator (JULES), Simple Water Balance Model (SWBM), and the simple conceptual HBV hydrological model (HBV-SIMREG) as data from the models was not available from the data portal for the selected basins at the time of writing. As such, seven models and model ensemble were included in this study. Evaluation of ET data also omits Lisflood model as data was not available from the portal at the time writing. Although there is an available Tier 2 product with a higher spatial resolution (0.25°), this study did not utilise these data as selected basins were not included at the time of conducting this research. We also evaluated discharge from FLDAS-Noah with spatial resolution of 0.1° and TerraClimate with a spatial resolution of 0.041° . Table 2 provides a brief summary of the different models used in this study.

Table 2: Water resources reanalysis (WRR) products evaluated

Model provider	Model name	Model type	Routing scheme	Reference
CNRS (Centre National de la Recherche Scientifique)	ORCHIDEE (Organizing Carbon and Hydrology in Dynamic Ecosystems)	LSM	Cascade of linear reservoirs	(Krinner et al., 2005)
CSIRO (Commonwealth Scientific and Industrial Research Organization)	AWRA-L (Australian Water Resources Assessment)	GHM	Cascade of linear reservoirs	(Van Dijk et al., 2014)
ECMWF (European Centre for Medium-Range Weather Forecasts)	HTESSEL (Hydrology Tiled ECMWF Scheme for Surface Exchanges over Land)	LSM	CaMa-Flood	(Balsamo et al., 2009)
JRC (Joint Research Centre)	LISFLOOD	GHM	Double kinematic wave	(Van Der Knijff et al., 2010)
UniUt (Universiteit Utrecht)	PCR-GLOBWB	GHM	Travel time	(Van Beek et al., 2011)
MeteoFr (Meteo France)	SURFEX	LSM	TRIP with stream	(Decharme et al., 2010)
UniK (Universitat Kassel)	WaterGAP	GHM	Manning–Strickler	(Wada et al., 2014)
NASA	Noah	LSM	Soil-layer water and energy balance	(McNally et al., 2017)
University of California Merced	TerraClimate	GHM	Bucket type model	(Abatzoglou et al., 2018)

168

2.2.2. Evapotranspiration products

169
170 In addition to the ET estimates from the reanalysis products, we also evaluated several satellite-based
171 ET estimates including GLEAM3.5a & 3.5b, MODIS16A2, PMLV1, PMLV2, SSEBop, (see Table
172 3). ET products from WRR have the same spatial resolution with the discharge estimates while remote
173 sensing products have different spatial resolutions. However, we did not resample the data to the same
174 resolution because a previous study has shown that resampling does not have any significant impact
175 on the results (Weerasinghe et al., 2020). Table 3 provides a summary of all ET products evaluated
176 in this study.

177 **Table 3: Summary of the characteristics of the different ET products**

ET product	Core equation	Temporal resolution	Spatial resolution	References
GLEAM3.5a & 3.5b	Priestley-Taylor	Monthly	0.25° x 0.25°	(Martens et al., 2017)
MODIS16A2	Penman-Montieth	8-day	1/48°x1/48°	(Mu et al., 2007; Mu et al., 2011)
PMLV1	Penman-Monteith-Leuning	Monthly	0.5° x 0.5°	(Zhang et al., 2016)
PMLV2	Penman-Monteith-Leuning	8-day	1/192°x1/192°	(Zhang et al., 2019)
SSEBop	Surface Energy Balance	Monthly	1/96° x 1/96°	(Senay et al., 2013)
CR-ET	Penman-Montieth	Monthly	0.25°	(Ma et al., 2021)

2.3. Evaluation data

2.3.1. River discharge

178
179
180
181 Observed river discharge data were used to evaluate the performance of WRR models and to estimate
182 basin-wide water balance evapotranspiration (ET_{WB}) using the water balance concept. The source of
183 the river discharge data is available in Table 1. Gaps in the discharge data were filled using Self-
184 Organizing Maps which have been shown to be a robust method for infilling missing gaps in
185 hydrometeorological time series (Nkiaka et al., 2016).

2.3.2. Precipitation

186
187 Climate Hazards Group InfraRed Precipitation with Station data (CHIRPS) was used to estimate
188 ET_{WB} . CHIRPS has a quasi-global coverage at a spatial resolution of 0.05° x 0.05°, spanning the
189 period from 1981 to the present at a daily timescale (Funk et al., 2015). The dataset was designed
190 taking into consideration the weaknesses of existing products (Sulugodu et al., 2019). As such,
191 CHIRPS blends gauge and satellite precipitation covering most global land regions, it has low latency,
192 high resolution, low bias, and long period of record (Funk et al., 2015). CHIRPS has extensively been
193 validated (Dinku et al., 2018; Satgé et al., 2020) and used in several studies in Africa (Larbi et al.,
194 2021; Nkiaka, 2022). The data was downloaded as the spatial average for each basin using the climate
195 engine App and used to estimate ET_{WB}

196
197
198
199
200
201
202
203
204
205
206
207
208
209
210
211
212
213
214
215
216
217
218
219
220
221
222
223
224
225
226
227

2.3.3. GRACE

GRACE data are monthly anomalies of terrestrial water storage changes (TWSC) used to quantify changes in terrestrial water storage. The dataset has a global coverage spanning the period 2003–2017 (Tapley et al., 2019). The data was derived from Jet Propulsion Laboratory (JPL) RL06M Version 2.0 GRACE mascon solution at a spatial resolution of $0.5^\circ \times 0.5^\circ$. The data has a coastline resolution improvement (CRI) filter to reduce leakage errors across coastlines and land-grids, using scaling factors derived from the community land model (Wiese et al., 2016). GRACE data has recently been re-processed to reduce measurement errors and represents a new generation of gravity solutions that do not require empirical post-processing to remove correlated errors, as such, the present data is better than the previous GRACE version that was based on spherical harmonic gravity solution (Wiese et al., 2016). GRACE data was used in this study to estimate ET_{WB} following the approach used in other studies e.g., (Andam-Akorful et al., 2015; Liu, 2018; Xie et al., 2022).

2.4. Evaluating gridded WRR

WRR models were evaluated following a multi-objective approach commonly used in evaluating the performance of hydrological models, including the Nash-Sutcliffe efficiency (NSE), Kling-Gupta efficiency (KGE), and the percent bias (PBIAS). NSE scores range from $-\infty$ to 1, with 1 indicating a perfect representation of observed discharge. NSE scores ≥ 0.50 can be considered acceptable whereas NSE scores ≤ 0.0 indicate poor model performance (Moriasi et al., 2007). Similarly, the KGE is a dimensionless metric that can be decomposed into three components crucial for evaluating hydrological model performance accounting for temporal dynamics (correlation), bias errors (observed vs simulated volumes), and variability errors (relative dispersion between observations and simulations) (Gupta et al., 2009). KGE scores range from $-\infty$ to 1, with 1 considered the ideal value. Next, PBIAS is used to measure the tendency of the simulated discharge to be larger or smaller than their observed counterparts (Gupta et al., 2009). PBIAS is expected to be 0.0, with low magnitude values indicating accurate simulations, positive values indicate underestimation, negative values indicate overestimation (Moriasi et al., 2007). According to Moriasi et al. (2007), a hydrological model with PBIAS values in the range $\pm 25\%$ can be considered to be acceptable. Furthermore, a temporal evaluation of flow hydrographs was carried out by plotting the monthly simulated vs observed discharge to ascertain visually if the models were able to capture the magnitude, seasonality, and interannual variability of discharge.

Table 4: Contingency table for 80th percentile river discharge

	Observed discharge	
	Yes	No
Simulated discharge	Yes	Hits (H) False Alarms (FA)
	No	Misses (M) Correct Negatives

228 Lastly, we evaluated the models ability to predict discharge above specific thresholds. This evaluation
 229 step is of critical importance when considering operational water management requirements such as
 230 water allocation and reservoir operation which rely on monthly river discharge. To achieve this, we
 231 adopted the Critical Success Index (CSI) as the metric to evaluate the ability of each model to simulate
 232 discharge exceeding the 20th and 80th percentiles. CSI is calculated from a two-dimensional
 233 contingency table defining the events in which observed and simulated discharges exceed a given
 234 threshold (Thiemig et al., 2015). We used the 20th and 80th percentiles to assess the ability of the
 235 models to simulate both low and high flows respectively. The contingency table (Table 4) is a
 236 performance measure used in summarizing all possible forecast-observation combinations such as
 237 hits (H; event forecasted and observed), misses (M; event observed but not forecasted), false alarms
 238 (FA; event forecasted but not observed) and correct negatives (CN; event neither forecasted nor
 239 observed). The ideal value for CSI is 100% and the metric is calculated as follows:

$$240 \quad CSI = \frac{H}{H + M + FA} \times 100 \quad (1)$$

241 **2.5. Evaluating gridded ET**

242 We also adopted a multi-step approach to evaluate the performance of ET products by assessing the
 243 annual ET–precipitation ratio, evaluating the statistical performance of ET products against long-term
 244 ET_{WB} and the ability of the products to capture monthly ET variability.

245 In the first step, the annual ET–precipitation ratio was calculated to compare with the ratio
 246 obtained using ET_{WB} method. The ET–precipitation ratio can also provide an estimate of the amount
 247 of water available in each basin after evapotranspiration losses. In the second step, different statistical
 248 metrics were used to assess the performance of the ET products using the monthly ET_{WB} as a reference
 249 (Andam-Akorful et al., 2015; Burnett et al., 2020; Koukoula et al., 2020). The monthly ET_{BW} was
 250 calculated using the basin water balance equation as follows:

$$251 \quad ET_{WB} = P - Q - \Delta S \quad (2)$$

252 Where P is average monthly precipitation over the basin (mm), Q is river discharge (mm) and ΔS is
 253 the terrestrial water storage change [TWSC] (mm). Unlike several studies that have evaluated ET
 254 products on an annual timescale, this study adopts a monthly sample. As such, the TWSC component
 255 (ΔS) in equation 2 that is often neglected when estimating ET_{WB} over several years (≥ 10 years) could
 256 not be overlooked. Due to the likely impact of anthropogenic activities such as reservoir operation,
 257 water withdrawal, and monthly rainfall variability on TWSC, values derived at monthly timescales
 258 are important. In this case, TWSC data used in this study were obtained from GRACE.

259 Due to the coarse spatial resolution of GRACE, it has been argued that GRACE is not sensitive
 260 at detecting changes in monthly TWSC in small-size basins $\leq 150,000 \text{ km}^2$ (Rodell et al., 2011). Based
 261 on this claim, it might be argued that GRACE data may not be applicable in this study considering
 262 that most of the basins are below this threshold except the Oubangui ($499,000 \text{ km}^2$). However, several
 263 studies (Liu, 2018; Biancamaria et al., 2019; Oussou et al., 2022; Xie et al., 2022), have demonstrated
 264 that GRACE can provide acceptable TWSC estimates for basins that are smaller than this threshold.
 265 Encouraging results from these and other studies do therefore suggest that GRACE data can be used
 266 in this study; albeit with the expectation of considerable uncertainties in TWSC estimates. For this
 267 study, GRACE data for each basin were obtained by averaging the timeseries of all coincident
 268 GRACE grid cells. To estimate changes in monthly TWSC, we calculated the difference between
 269 consecutive GRACE measurements for each basin, divided by the time between measurements, using
 270 the following equation:

$$271 \quad \Delta S = (S_{[n]} - S_{[n-1]})/dt \quad (3)$$

272 where ΔS represents the TWSC (mm), n is the measurement number, and dt is the time difference
 273 between two consecutive GRACE measurements (months).

274 Lastly, temporal evaluation of the products was carried out by plotting the time series of all
 275 ET products against ET_{WB} to visually establish if the gridded ET products were able to capture the
 276 magnitude, seasonality, and interannual variability of ET across the basins.

277 **2.6. Estimating relative uncertainty in basin-scale water balance ET (ET_{WB})**

278 To estimate the relative uncertainty in monthly ET_{WB} , we first calculated the absolute uncertainty in
 279 monthly ET_{WB} by propagating errors through each of the components in equation 2 (Rodell et al.,
 280 2011), as follows:

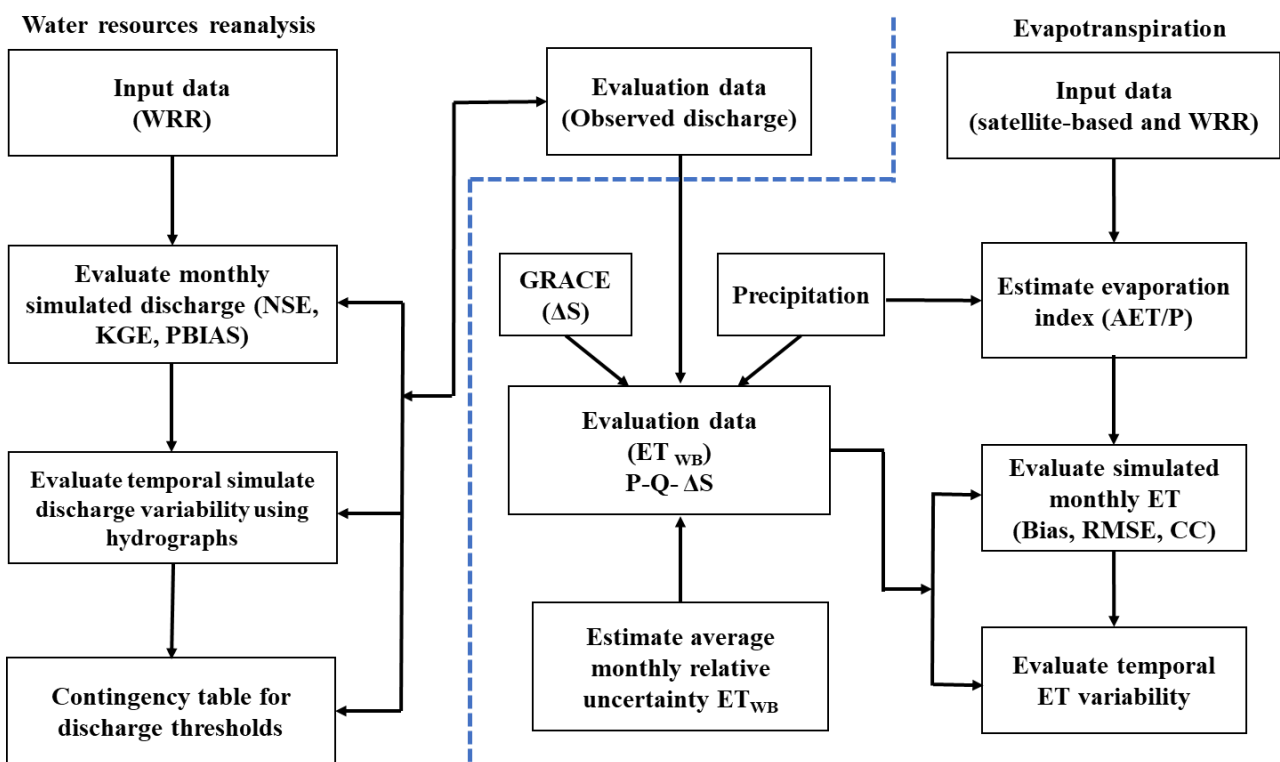
$$281 \quad \sigma_{ET} = \sqrt{\sigma_P^2 + \sigma_Q^2 + \sigma_{\Delta S}^2} \quad (4)$$

282 Where σ_P , σ_Q and $\sigma_{\Delta S}$ represent the absolute uncertainties in basin precipitation, observed river
 283 discharge, and TWSC respectively. Uncertainty in precipitation was estimated as systematic errors
 284 (bias). For this, we used a value of 2 % estimated for CHIRPS data at monthly timescale from 1981–
 285 2016 over Africa from a validation study using the Global Precipitation Climatology Centre (Shen et
 286 al., 2020). Uncertainty in TWSC was determined using the gridded fields of measurement and leakage
 287 errors (residual errors after filtering and rescaling) that are provided with the GRACE data. The
 288 uncertainty for each basin was calculated by averaging the values of all GRACE grid cells within
 289 each basin. To account for month-to-month variation in equation 3, the TWSC error values were

290 multiplied by $\sqrt{2}$ to obtain $\sigma_{\Delta S}$ (Andam-Akorful et al., 2015). Because no uncertainty estimates were
 291 provided with the river discharge data, we adopted a value of 20 % which has been used in a recent
 292 study in the region (Burnett et al., 2020). After calculating the absolute uncertainty in monthly ET_{WB} ,
 293 the relative monthly uncertainty was calculated using equation 5 (Baker et al., 2021) as follows:

$$294 \quad vET = \frac{\sigma ET}{ET_{WB}} \times 100 \quad (5)$$

295 Where vET is the monthly relative uncertainty (%), σET is the absolute monthly uncertainty (mm),
 296 and monthly ET_{WB} (mm). Figure 2 shows a flowchart detailing the different steps used for evaluating
 297 the WRR and ET products.



298
 299 **Figure 2:** Flowchart outlining the steps used in evaluating the WRR and ET products (The blue
 300 dotted line in the flow chart separates evaluation of WRR from ET products)

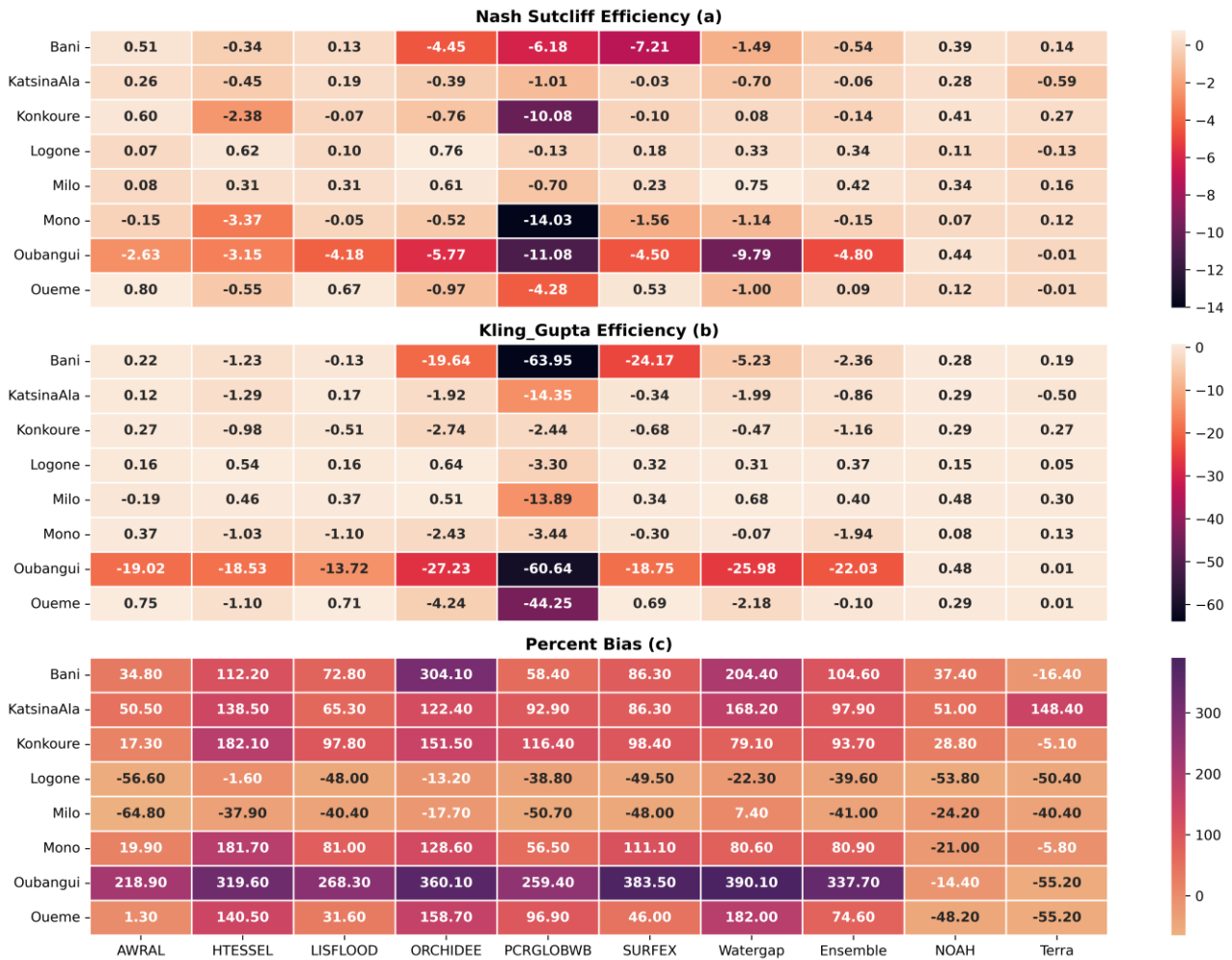
301 3. Results

302 3.1. Water resources reanalysis products

303 3.1.1. Hydrological performance

304 A multi-objective approach using different statistical metrics (NSE, KGE and PBIAS) was used to
 305 evaluate discharge estimates from WRR products. The performance of the models in simulating
 306 discharge is shown in Figure 3. Using the NSE as a performance metric, results show that Noah
 307 produced positive scores in all the basins (0.15–0.48). Terra, AWRAL and Lisflood produced positive
 308 scores (0.01–0.75) in seven, six and four basins respectively. SURFEX model produced positive

309 scores in three basins while ORCHIDEE, HTESSSEL, Watergap and the ensemble mean produced
 310 positive scores in two basins each while PCR-GLOBW produced negative scores in all the basins
 311 (Figure 3a).



312
 313 **Figure 3:** Statistical evaluation of the models using (a) NSE, (b) KGE, and (c) PBIAS. Red and
 314 orange colours represent poor model performance in Figures 3a, 3b & 3c, however, the acceptable
 315 PBIAS range in Figure 3c is $\pm 25\%$. Ensemble refers to the mean of WRR from the earthH2Observe.

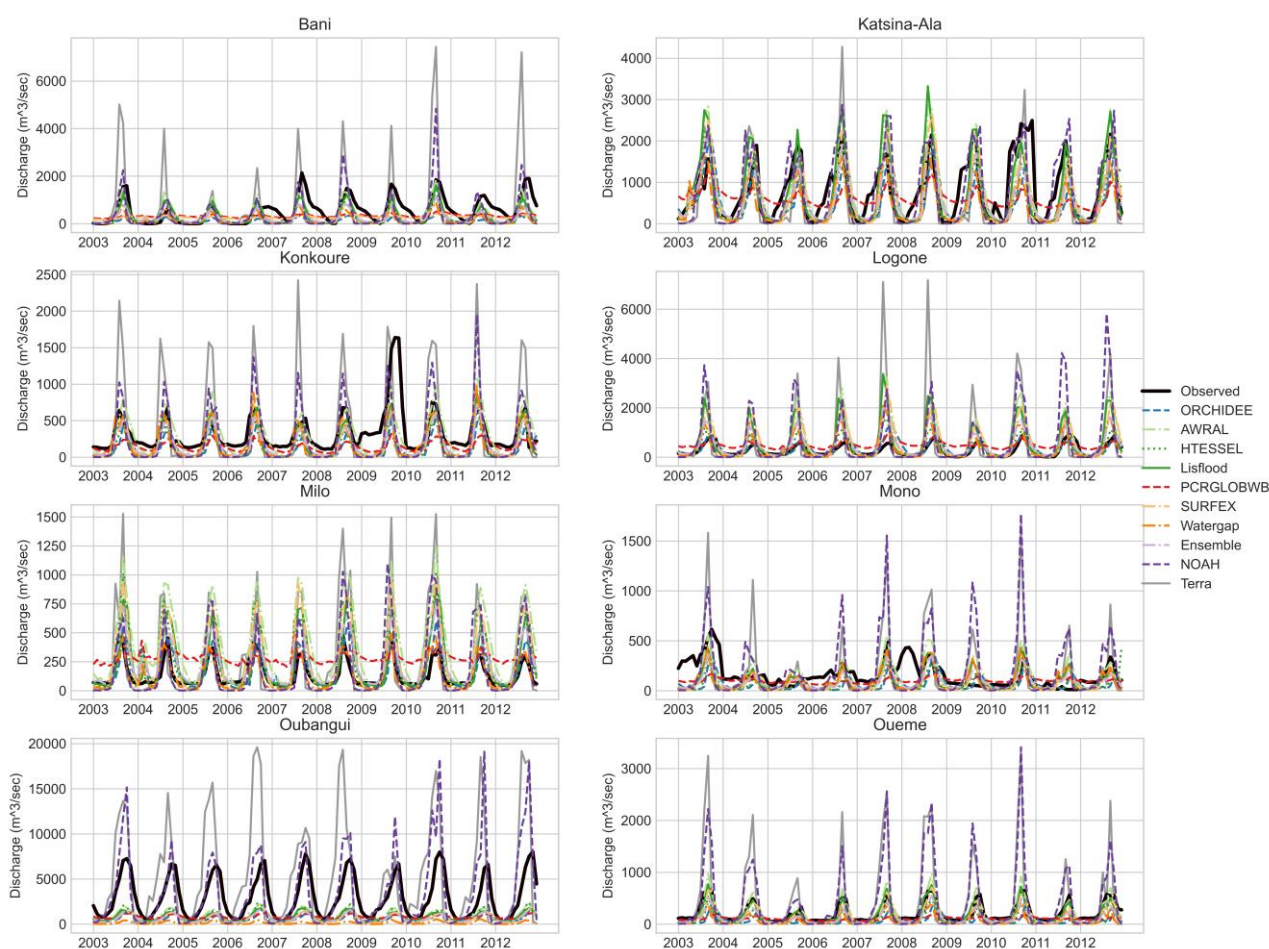
316 KGE results show that Noah also produced positive scores (0.11– 0.44) in all basins, followed by
 317 AWRAL, Lisflood and Terra with positive scores in six, five and four basins respectively (Figure
 318 3b). SURFEX and Watergap produced positive scores in three basins while ORCHIDEE and
 319 HTESSSEL produced positive scores (0.31–0.76) in two basins. The ensemble mean produced positive
 320 scores (0.09 – 0.42) in three basins while PCRGLOBW produced the lowest KGE scores (Figure 3b).

321 Positive and negative PBIAS values were obtained in the different basins. Negative values
 322 indicate that the model overestimated discharge volumes compared to observed discharge while
 323 positive values indicate the opposite. Noah, Terra and AWRAL produced acceptable PBIAS scores
 324 ($\pm 25\%$) in three basins, ORCHIDEE and Watergap produced similar scores in two basins and

325 HTESSEL in one basin (Figure 3c). The rest of the models including the ensemble mean either grossly
 326 overestimated or underestimated discharge volumes in all the basins.

327 3.1.2. Temporal evaluation

328 The ability of the models to capture discharge variability was analysed by comparing the simulated
 329 vs observed discharge. Results show that most of the models were able to capture the seasonal
 330 discharge variability including peak and low flows (Figure 4). However, PCR-GLOBW
 331 systematically overestimated low flows and underestimated high flows across all basins. In the
 332 Oubangui basin, all models were able to capture the seasonal variability but consistently
 333 underestimated peak flows except Noah and Terra models which overestimated peak flows (Figure
 334 4). For example, measured peak discharge in the river exceeds 5000 m³/sec, but all models except
 335 Noah and Terra simulated it to be less than 2000 m³/sec (Figure 4).

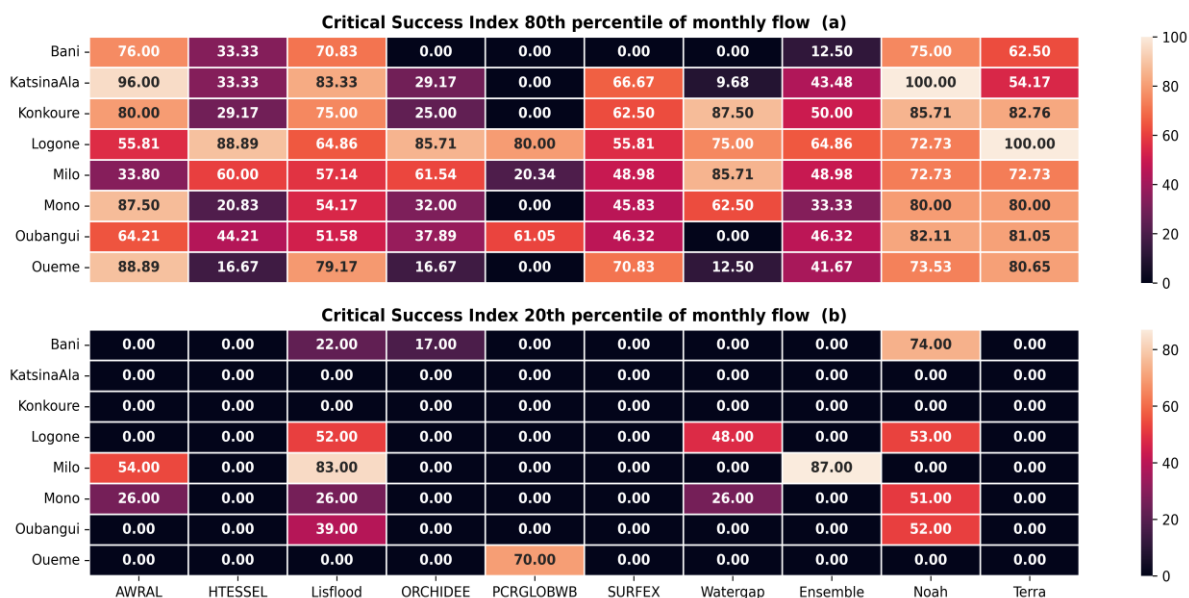


336
 337 **Figure 4:** Evaluation of temporal flow variability simulated by the different model

338 3.1.3. Critical Success Index

339 Figure 5 shows the performance of the models in simulating the 80th and 20th percentiles monthly
 340 discharge. For the 80th percentile flows, results show that Noah and Terra produced CSI scores above
 341 50 % in all basins followed by Lisflood and AWRAL in seven and six basins respectively while

342 Surfex and Watergap produced similar scores in four basins each (Figure 5a). For the 20th percentile
 343 flows, only Noah produced CSI scores above 50 % in four basins while Lisflood produced similar
 344 scores in two basins. The performance of the other models in simulating the 80th percentile flow
 345 shows a large spread while most models including the ensemble mean failed to simulate the 20th
 346 percentile flow across all the basins. Taking together, results suggest that the models simulated high
 347 flows better than the low flows with only Noah capable of capturing both flow regimes in most basins
 348 (Figure 5b).

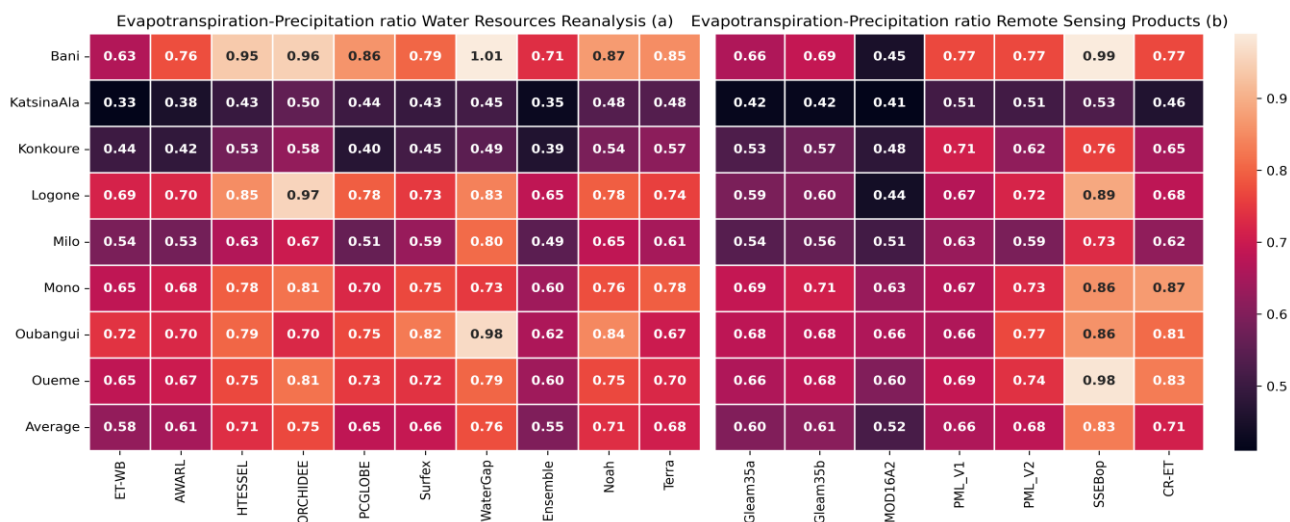


349 **Figure 5:** Critical Success Index for 80th and 20th percentile of monthly flow across all basins

351 3.2. Evapotranspiration products

352 3.2.1. Evapotranspiration–precipitation ratio

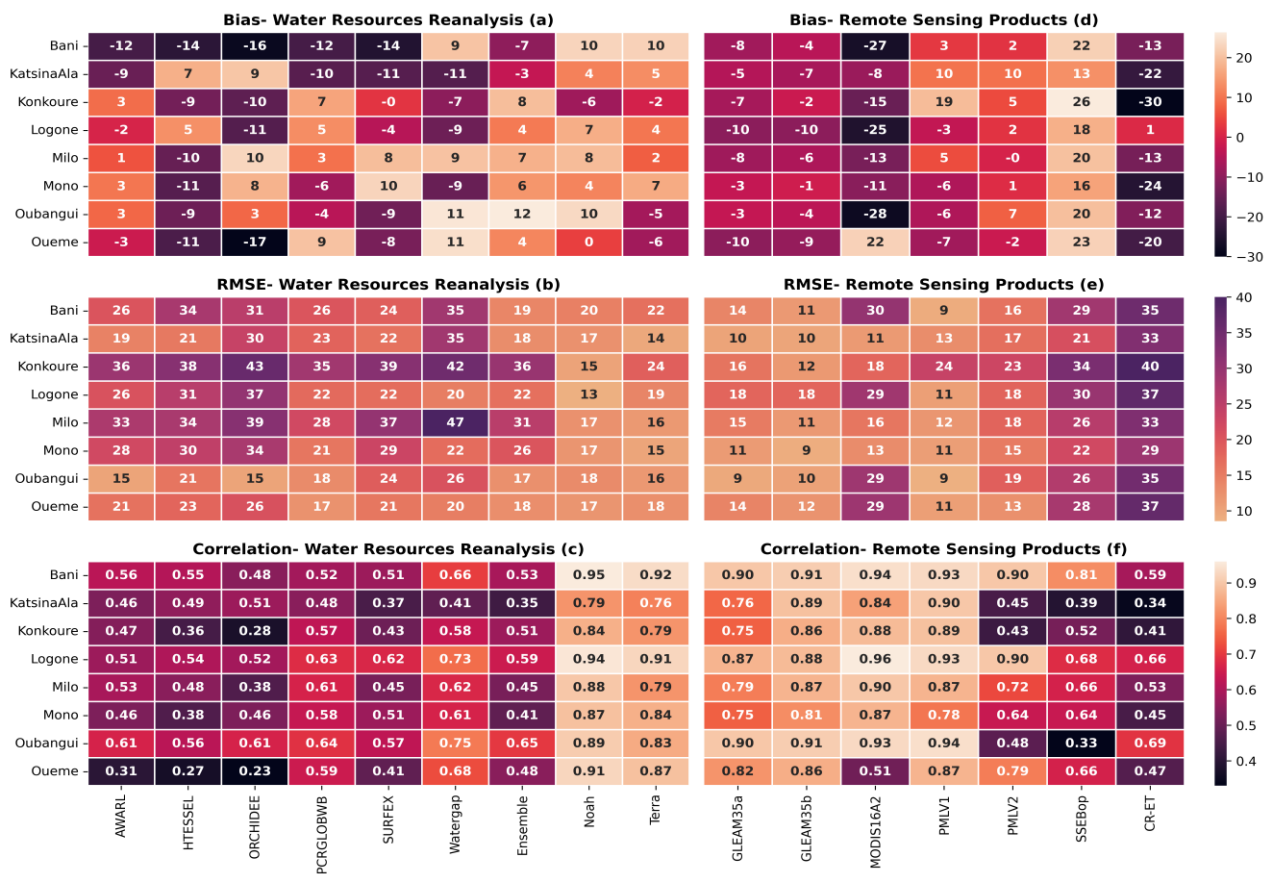
353 Figure 6 shows the annual ET–precipitation ratio for all basins. It can be observed that average annual
 354 ET–precipitation ratio ranges between (0.58–0.76) for WRR and (0.52–0.83) for satellite-based
 355 products over a period of 10 years (2003–2012) across all basins. WaterGap produced the highest
 356 ratio (0.45–1.01) among WRR models, SSEBop produced the highest ratio (0.53–0.99) while
 357 MOD16A2 produced the lowest ratio (0.41–0.66) among the satellite-based products (Figure 6).
 358 Results show that the evaporation ratios from the different ET estimates are in the same order of
 359 magnitude with the ratio from ET_{WB} across all the basins except for WaterGap, SSEBop, MOD16A2
 360 and CR-ET which produced values which were beyond this range (Figure 6).



361
362 **Figure 6:** Annual evapotranspiration – precipitation ratio 2003 – 2012

363 **3.2.2. Basin-wide water balance estimates**

364 Figure 7 shows the results of the statistical metrics used in evaluating the ET estimates using monthly
 365 ET_{WB} as reference. Considering bias as a performance metric, AWARL, Noah and Terra produced
 366 the lowest bias scores among the estimates from WRR while PMLV2, Terra, and GLEAM3.5a & 3.5b
 367 produced the lowest bias scores among the satellite-based products (Figure 7a&d). Most WRR
 368 products underestimated ET and similarly GLEAM also slightly underestimated ET, among the
 369 satellite-based products while the rest of the products produced mixed results (Figure 7a&d).
 370 However, SSEBop systematically overestimated ET in all the basins while MOD16A2 grossly
 371 underestimated this variable in all but one basin with respect to monthly ET_{WB} (Figure 7d).



372

373

374

Figure 7: Bias, RMSE, and Pearson correlation coefficient between monthly ET_{WB} and different ET products (a-c: WRR and d-f: remote sensing products).

375

376

377

378

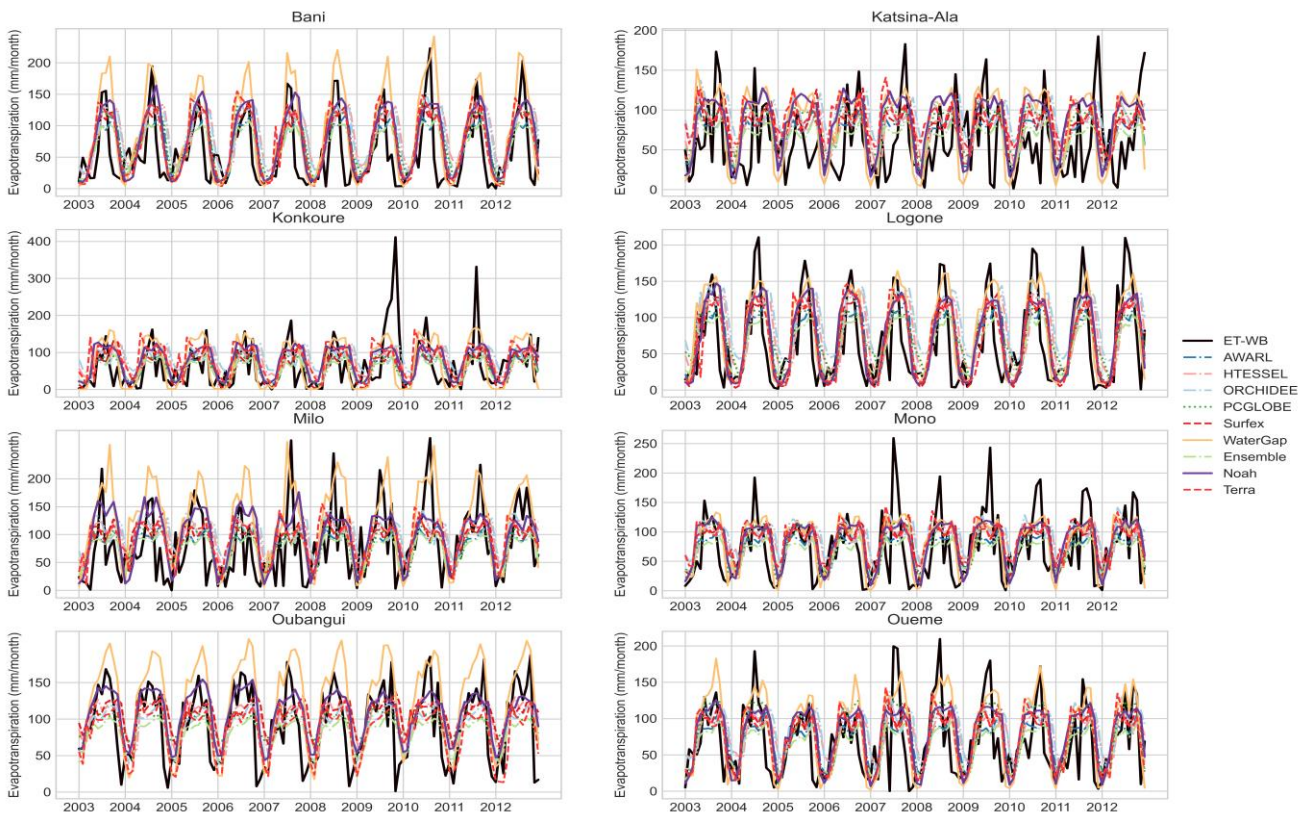
379

380

381

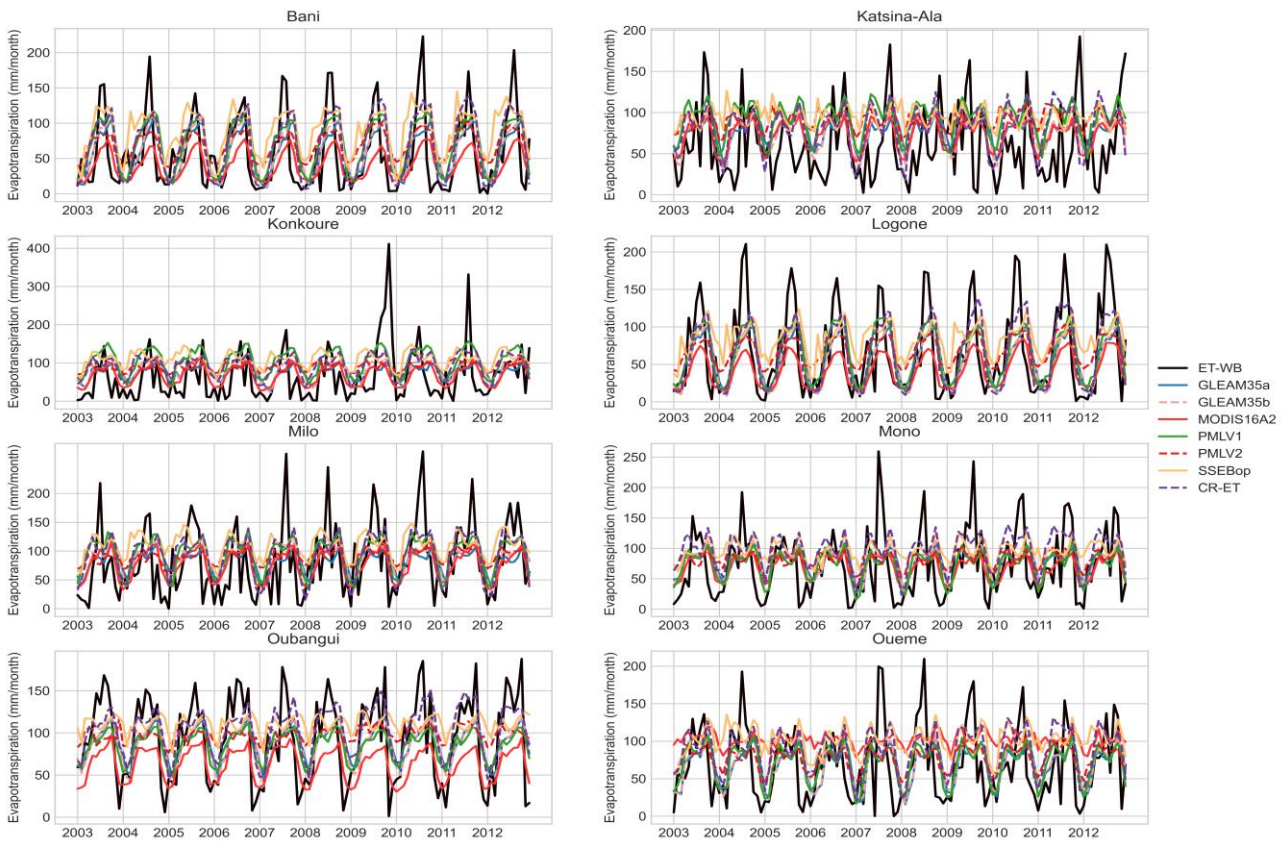
382

Noah produced the lowest RMSE (13–20 mm/month) among the WRR products while GLEAM3.5a & b and PMLV1 produced the lowest RMSE (8.50–12 mm/month) among the satellite-based products (Figure 7b&e). The rest of the products both WRR and satellite-based produced substantially higher RMSE scores (Figure 7b&e). Only Noah and Terra produced high Pearson correlation scores across all basins among WRR products (Figure 7c). On the other hand most satellite-based products produced high Pearson correlation scores (≥ 0.75) in all basins except PMLV2 and SSEBop which both produced low scores (< 0.50) in three and two basins respectively (Figure 7f). ET estimates produced from complimentary relationship (CR-ET) performed poorly across most basins.



383

384 **Figure 8a:** Seasonal cycle of ET estimates from WRR and basin-wide water balance
 385 evapotranspiration. ET_{WB} represents monthly evapotranspiration estimated by the water balance
 386 method, while the rest are derived from LSMs and GHMs.



387

388 **Figure 8b:** Seasonal cycle of ET estimates from remote sensing-based products and basin-wide water
 389 balance evapotranspiration.

3.2.3. Monthly ET variability

Figure 8 shows the seasonal cycle of ET_{WB} against both WRR products and satellite-based ET estimates. It can be observed that most products were able to replicate the seasonal ET cycle across all the basins (Figure 8a&b). In addition, most products were not able to replicate the high ET peaks produced by ET_{WB} during the rainy season except WaterGap in some instances (Figure 8a). The performance of CR-ET follows that of the rest of the products.

3.2.4. Estimating relative uncertainty in ET_{WB}

An assessment of absolute uncertainties in monthly ET_{WB} indicated that the dominant sources of uncertainty vary from one basin to another and by each month. For example, in the Katsina-Ala, Konkoure, and Milo basins, the dominant source of uncertainty in monthly ET_{WB} was river discharge (**supplementary material**). Although the absolute uncertainty in precipitation and TWS also appear to be high in the three basins, the uncertainty in river discharge takes precedence over the other sources of uncertainty due to its higher magnitude (**supplementary material**). On the contrary, the dominant source of uncertainty in ET_{WB} in the Bani, Logone, and Oubangui basins was from TWSC. Across all the basins, there was no significant variation in monthly TWSC uncertainty which is consistent with the results of a similar study in the Amazon basin (Baker et al., 2021). Results also revealed that the magnitude of TWSC uncertainty were similar across the basins irrespective of the basin size (**Supplementary material**).

Figure 9 shows the relative uncertainty in ET_{WB} across all the basins. It can be observed that relative uncertainty values are generally <30 % but vary from month to month. However, the values were exceptionally high in the Katsina-Ala and Konkoure basins. The relative uncertainty in ET_{WB} also appears to be exceptionally high in the months of September–November which corresponds to the high flow season across most basins. Taking together, the average monthly relative uncertainty in ET_{WB} for all basins ranges from 10–18% except in the Katsina-Ala and Konkoure basins where this range is grossly exceeded.

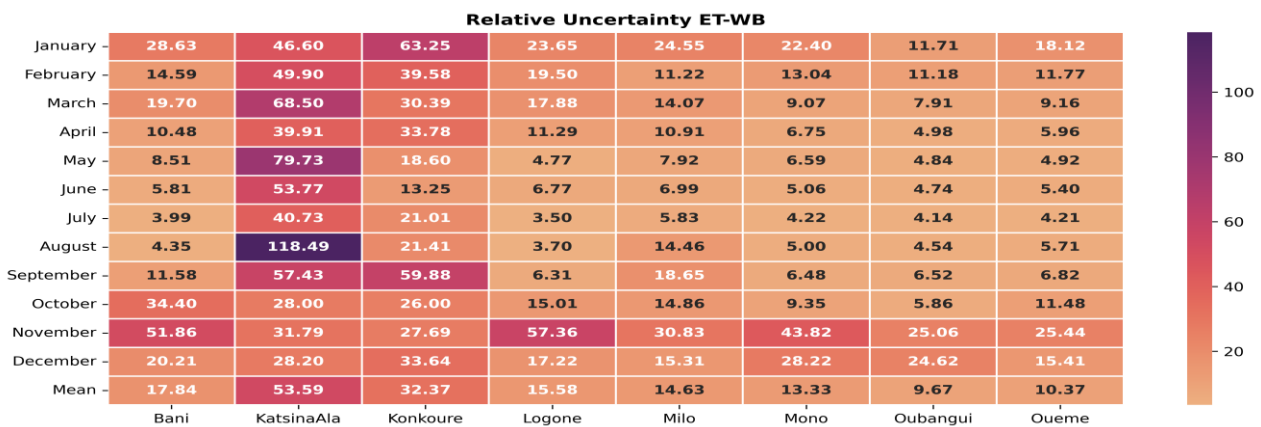


Figure 9: Average (2003 – 2012) monthly relative uncertainty in monthly ET_{WB} (%)

417 **4. Discussion**

418 The overarching goal of this paper was to assess the performance of gridded water resources
419 reanalysis and evapotranspiration products and to estimate the relative uncertainty in monthly basin-
420 wide evapotranspiration (ET_{WB}) estimates. Below we provide a discussion and implications of our
421 results in water security assessment in ungauged basins.

422 **4.1. Water resources reanalysis**

423 The performance of WRR products was assessed through commonly used model evaluation metrics,
424 discharge variability, and verification skill scores (critical success index) using observed river
425 discharge data. Our results show strong differences in the performance of the different models in
426 simulating river discharge across the basins. Noah model produced positive NSE and KGE values in
427 all basins and PBIAS values within the acceptable range ($\pm 25\%$) in three basins. Temporal evaluation
428 of the WRR products showed that Noah, Terra, AWRAL and Lisflood were able to capture the
429 seasonal variability in discharge as demonstrated by high KGE scores. Indeed, high KGE values
430 suggest that some models were able to capture the temporal dynamics (strong correlation), and low
431 bias scores indicate that the variability errors between the observed discharge and simulation was also
432 low (Gupta et al., 2009). Nevertheless, Terra consistently overestimated peak flows in all the basins.

433 Apart from Noah model which is a LSM used in FLDAS, most GHMs used in
434 earthH2Observe tier 1 product performed better than the LSMs, which is consistent with results from
435 other studies (Lakew et al., 2020). The strong performance of GHMs compared to LSMs can be
436 attributed to the differences in the model structure and parametrisation schemes between LSMs and
437 GHMs (Gründemann et al., 2018; Koukoula et al., 2020). For example, some GHMs such as
438 Watergap are able to simulate lakes and reservoirs and water withdrawal while LSMs can only
439 simulate natural processes. Such differences in model structure can significantly influence discharge
440 volumes simulated by both types of models (Gründemann et al., 2018). Although PCRGLOBW is a
441 GHM, it produced substantially low performance compared to the LSMs which is consistent with
442 results from other studies in the region (Gründemann et al., 2018; Lakew et al., 2020). This suggest
443 that PCRGLOBW model may not be suitable for assessing water security in the region.

444 The ability of the models to simulate flow thresholds was evaluated using the CSI. Results
445 show that Noah, Terra, AWRAL and Lisflood were able to capture more than 50% of 80th percentile
446 monthly flow in most basins. We also noted that apart from Noah model, the rest of the GHMs
447 performed better than the LSMs from earthH2Observe in their ability to capture the 80th percentile
448 monthly flows across the basins while only Noah was able to capture 20th percentile flows in three
449 basins. The performance of Noah compared to other models can be attributed to the fact that FLDAS
450 was specially designed and optimized to produce physically meaningful variables for monitoring food

451 and water security in data-scarce regions in Africa (McNally et al., 2017). Furthermore, Noah and
452 Terra with spatial resolutions of 0.1° & 0.041° respectively perform better than other models and this
453 may be attributed to their higher spatial resolutions compared to other models with coarser resolution
454 (0.5°). In fact, Gründemann et al. (2018), has shown that WRR products with higher spatial resolution
455 perform better than products with coarser resolution in their ability to simulate discharge. The
456 performance of Noah can also be attributed to the fact the FLDAS is driven by a combination of
457 different precipitation products thereby reducing the uncertainty in the input data while earth2observe
458 tier 1 product are driven by only one data source (WFDEI) which increases the uncertainty in the
459 input data which is propagated to the model outputs. Our results also showed that Lisflood performed
460 better than most other earth2observe models and this can be attributed to the fact that Lisflood has
461 been extensively used in research and operational settings in Africa (Thiemig et al., 2015; Smith et
462 al., 2020). As such, the model parameters may have been better constrained in the region than other
463 models from earth2Observe. Taking together, results from this study highlight the importance of
464 evaluating outputs from WRR products in representative basins before applying them in studies that
465 may have wider policy and financial implications. Our results suggest a need to enhance the spatial
466 resolution of WRR products and for the products to be driven by input data from multiple sources to
467 reduce the uncertainties input data.

468 **4.2. Evapotranspiration products**

469 The annual ET–precipitation ratio produced by WRR and satellite-based ET products are within the
470 range estimated for the global land regions (Rodell et al., 2015) with the only exception being
471 WaterGap, SSEBop, MOD16A2 and CR-ET with values beyond this range. This suggests that ET
472 estimates from both sources performed well in this aspect of the ET evaluation. The annual ET–
473 precipitation ratios obtained in this study suggests that annual ET does not exceed annual precipitation
474 in most basins during the period under evaluation. This suggest the availability of sufficient water
475 resources in each basin.

476 Considering all the ET evaluation criteria and comparing between estimates from WRR and
477 satellite-based products, Noah, Terra, GLEAM3.5a & 3.5b, and PMLV2 appear to outperform the
478 rest of products even though GLEAM products slightly underestimated ET in all the basins.
479 Conversely, WaterGap, SSEBop and MOD16A2 performed poorly and may not be suitable for water
480 security assessment in the region. Our results are generally consistent with those from other studies
481 indicating that GLEAM and MODIS16A2 underestimate evapotranspiration, while SSEBop
482 overestimates this variable in most parts of Africa (Weerasinghe et al., 2020; Adeyeri and Ishola,
483 2021; Mcnamara et al., 2021). Given that ET estimates from Noah and Terra are produced together
484 with other water balance components (runoff, soil moisture and baseflow) the two models may be

485 recommended for water security assessment in the region because of water balance closure. Our
486 results also revealed that the performance of satellite-based ET products is not influence by spatial
487 resolution which is consistent with results from previous studies (Weerasinghe et al., 2020; Jiang and
488 Liu, 2021). For example, Gleam products with a spatial resolution of 0.25° outperformed products
489 such as MODIS16A2 and SSEBop with higher spatial resolutions. On the contrary, ET estimates
490 from WRR appear to be influenced by spatial resolution considering that Noah and Terra with higher
491 spatial resolutions perform better than other products with coarser resolutions.

492 Although all the products were able to capture the temporal dynamics of ET in all the basins,
493 there were substantial differences in the magnitude of monthly ET from each model. This finding is
494 consistent with results from other studies showing strong differences in ET estimates produced by
495 different models (Weerasinghe et al., 2020; Adeyeri and Ishola, 2021). The discrepancies in monthly
496 ET estimates from the models may be attributed to differences model structure, parameters, and
497 uncertainties in the input data used in driving the models. This is also in-line with findings from
498 another study in West Africa highlighting the impact of model parameters and input data uncertainty
499 on ET estimates (Jung et al., 2019). Considering the aforementioned factors, it may be difficult to
500 expect the products to produce similar results. ET_{WB} estimates across all the basins produced high
501 peaks during the rainy season which is also similar to the results of a related study in West Africa
502 (Andam-Akorful et al., 2015). The high peaks observed in ET_{WB} may be attributed to errors inherent
503 in monthly precipitation, river discharge, and TWSC estimates used in estimating monthly ET_{WB} .

504 Given that there was no uncertainty information on the river discharge data used in this study,
505 we adopted a value of 20 % following a previous study in the region (Burnett et al., 2020). In fact,
506 we feel that this value may be conservative considering that uncertainties in river discharge in tropical
507 regions have been shown to exceed 200 % (Kiang et al., 2018). The mean monthly relative uncertainty
508 for ET_{WB} for most basins appears to be in the same order of magnitude (16 %) with results obtained
509 in the Amazon basin (Baker et al., 2021). Results also showed that the relative uncertainty in ET_{WB}
510 is not influenced by basin size as most basins produced similar (same order of magnitude) uncertainty
511 estimates. The relative uncertainty in monthly ET_{WB} was higher during the rainy season. This can be
512 linked to high rainfall input during the rainy season which translates to high river discharge and
513 TWSC thereby increasing the absolute uncertainties in the different water balance components used
514 in estimating ET_{WB} . Results from this study suggest that the relative the uncertainty in monthly ET_{WB}
515 may be substantial which can potentially influence the performance of ET products when they are
516 evaluated using the ET_{WB} method. We therefore recommend that evaluating the performance of ET
517 products at monthly timescale should be accompanied with the estimataion of relative uncertainties.

518

519 **5. Conclusions**

520 The objectives of this study were to assess the performance of water resources reanalysis and
521 evapotranspiration products and to estimate the relative uncertainties in monthly ET_{WB} across eight
522 basins in Africa. Results show varying strengths and weaknesses for the different models. Some
523 models were able to capture the river discharge dynamics in the basins while other models could not
524 adequately capture this pattern. Differences in the model performance can be attributed to differences
525 model structure, parameters, input data used in driving the models and the spatial resolution of the
526 WRR products. Apart from Noah which is a land surface model (LSM), global hydrological models
527 (GHMs) performed better than LSMs except PCRGLOBW.

528 Evaluation of gridded ET products also revealed varying strengths and weaknesses for the
529 different products. Based on the different evaluation criteria (bias, RMSE, Pearson correlation
530 coefficient, and temporal ET variability), Noah appears to outperform most of other ET estimates and
531 may therefore be recommended for water security assessment in the region. More so, because of water
532 balance closure and the availability of other water balance components (runoff, soil moisture and
533 baseflow). Our results also suggest that the performance of satellite-based ET products is not
534 influenced by spatial resolution, while differences in ET estimates may be attributed to differences in
535 model structure, parameters and the input data used to drive each model. On the contrary, spatial
536 resolution appear to have a significant impact on the performance of WRR in simulating ET estimates.

537 Our results also revealed that the relative uncertainties in monthly ET_{WB} were substantially
538 higher during the rainy season which can be attributed to uncertainties inherent in higher rainfall
539 leading to an increase in discharge magnitude and TWSC during this period. Results also revealed
540 that uncertainty in river discharge is the dominant source of uncertainty in ET_{WB} . This underscores
541 the need to prioritize the installation of new gauging stations while upgrading existing stations. This
542 is because uncertainties in river discharge could constrain the ability to fully understand hydrologic
543 variability and undermine discharge prediction.

544 Results from this study suggest that WRR and ET products may be used for water security
545 assessment in ungauged basins. However, it is imperative to evaluate the performance of these
546 products in representative gauged basins before applying them in ungauged basins. This is because
547 applying the products in ungauged basins without evaluating their performance may lead to poor
548 water management decisions with wider policy and financial implications. However, there is also a
549 need for WRR and ET products to be driven by input data from multiple sources to reduce
550 uncertainties in the input data and at the same time, the spatial resolution of WRR products needs to
551 be enhanced. Results from this study may be used by the products developers to improve on the
552 quality of future generations of WRR and ET products.

553 **Author contributions:** EN and RGB designed the methodological framework and contributed to the
554 entire strategic and conceptual framework of the study. EN prepared the data, performed the analyses,
555 interpreted the results and wrote the original draft. JN and EIB provided discharge data for the Mono
556 and Oueme basins respectively. All authors read the paper and provided feedback.

557 **Competing interests:** The authors declare that they have no conflict of interest.

558 **Acknowledgements:** E.N. was funded by the Leverhulme Trust Early Career Fellowship – Award
559 Number ECF–097–2020. We are grateful to Coralie Adams at Manchester University for writing the
560 Python code that was used to produce Figures 4 & 8.

561 **References**

- 562 Abatzoglou, J. T., Dobrowski, S. Z., Parks, S. A., and Hegewisch, K. C.: TerraClimate, a high-
563 resolution global dataset of monthly climate and climatic water balance from 1958–2015,
564 Scientific data, 5, 1-12, <https://doi.org/10.1038/sdata.2017.191>, 2018.
- 565 Adeyeri, O. E. and Ishola, K. A.: Variability and Trends of Actual Evapotranspiration over West
566 Africa: The Role of Environmental Drivers, Agricultural and Forest Meteorology, 308-309,
567 108574, <https://doi.org/10.1016/j.agrformet.2021.108574>, 2021.
- 568 Andam-Akorful, S. A., Ferreira, V. G., Awange, J. L., Forootan, E., and He, X. F.: Multi-model and
569 multi-sensor estimations of evapotranspiration over the Volta Basin, West Africa,
570 International Journal of Climatology, 35, 3132-3145, <https://doi.org/10.1002/joc.4198>, 2015.
- 571 Baker, J. C., Garcia-Carreras, L., Gloor, M., Marsham, J. H., Buermann, W., da Rocha, H. R., Nobre,
572 A. D., de Araujo, A. C., and Spracklen, D. V.: Evapotranspiration in the Amazon: spatial
573 patterns, seasonality, and recent trends in observations, reanalysis, and climate models,
574 Hydrology and Earth System Sciences, 25, 2279-2300, [https://doi.org/10.5194/hess-25-2279-
575 2021](https://doi.org/10.5194/hess-25-2279-2021), 2021.
- 576 Balsamo, G., Beljaars, A., Scipal, K., Viterbo, P., van den Hurk, B., Hirschi, M., and Betts, A. K.: A
577 revised hydrology for the ECMWF model: Verification from field site to terrestrial water
578 storage and impact in the Integrated Forecast System, Journal of hydrometeorology, 10, 623-
579 643, <https://doi.org/10.1175/2008JHM1068.1>, 2009.
- 580 Biancamaria, S., Mballo, M., Le Moigne, P., Sánchez Pérez, J. M., Espitalier-Noël, G., Grusson, Y.,
581 Cakir, R., Häfliger, V., Barathieu, F., Trasmonte, M., Boone, A., Martin, E., and Sauvage, S.:
582 Total water storage variability from GRACE mission and hydrological models for a 50,000
583 km² temperate watershed: the Garonne River basin (France), Journal of Hydrology: Regional
584 Studies, 24, 100609, <https://doi.org/10.1016/j.ejrh.2019.100609>, 2019.
- 585 Blatchford, M. L., Mannaerts, C. M., Njuki, S. M., Nouri, H., Zeng, Y., Pelgrum, H., Wonink, S., and
586 Karimi, P.: Evaluation of WaPOR V2 evapotranspiration products across Africa,
587 Hydrological processes, 34, 3200-3221, <https://doi.org/10.1002/hyp.13791>, 2020.
- 588 Burnett, M. W., Quetin, G. R., and Konings, A. G.: Data-driven estimates of evapotranspiration and
589 its controls in the Congo Basin, Hydrol. Earth Syst. Sci., 24, 4189-4211,
590 <https://doi.org/10.5194/hess-24-4189-2020>, 2020.
- 591 Byers, E., Gidden, M., Leclère, D., Balkovic, J., Burek, P., Ebi, K., Greve, P., Grey, D., Havlik, P.,
592 and Hillers, A.: Global exposure and vulnerability to multi-sector development and climate
593 change hotspots, Environmental Research Letters, 13, 055012, [https://doi.org/10.1088/1748-
594 9326/aabf45](https://doi.org/10.1088/1748-9326/aabf45), 2018.
- 595 Couasnon, A., Eilander, D., Muis, S., Veldkamp, T. I., Haigh, I. D., Wahl, T., Winsemius, H. C., and
596 Ward, P. J.: Measuring compound flood potential from river discharge and storm surge
597 extremes at the global scale, Natural Hazards and Earth System Sciences, 20, 489-504,
598 <https://doi.org/10.5194/nhess-20-489-2020>, 2020.

599 Decharme, B., Alkama, R., Douville, H., Becker, M., and Cazenave, A.: Global Evaluation of the
600 ISBA-TRIP Continental Hydrological System. Part II: Uncertainties in River Routing
601 Simulation Related to Flow Velocity and Groundwater Storage, *Journal of*
602 *Hydrometeorology*, 11, 601-617, <https://doi.org/10.1175/2010JHM1212.1>, 2010.

603 Dinku, T., Funk, C., Peterson, P., Maidment, R., Tadesse, T., Gadain, H., and Ceccato, P.: Validation
604 of the CHIRPS satellite rainfall estimates over eastern Africa, *Quarterly Journal of the Royal*
605 *Meteorological Society*, 144, 292-312, <https://doi.org/10.1002/qj.3244>, 2018.

606 Flörke, M., Schneider, C., and McDonald, R. I.: Water competition between cities and agriculture
607 driven by climate change and urban growth, *Nature Sustainability*, 1, 51-58,
608 <https://doi.org/10.1038/s41893-017-0006-8>, 2018.

609 Funk, C., Peterson, P., Landsfeld, M., Pedreros, D., Verdin, J., Shukla, S., Husak, G., Rowland, J.,
610 Harrison, L., and Hoell, A.: The climate hazards infrared precipitation with stations—a new
611 environmental record for monitoring extremes, *Scientific data*, 2, 1-21, 2015.

612 Gründemann, G. J., Werner, M., and Veldkamp, T. I.: The potential of global reanalysis datasets in
613 identifying flood events in Southern Africa, *Hydrology and Earth System Sciences*, 22, 4667-
614 4683, <https://doi.org/10.1038/sdata.2015.66>, 2018.

615 Gupta, H. V., Kling, H., Yilmaz, K. K., and Martinez, G. F.: Decomposition of the mean squared
616 error and NSE performance criteria: Implications for improving hydrological modelling,
617 *Journal of Hydrology*, 377, 80-91, <https://doi.org/10.1016/j.jhydrol.2009.08.003>, 2009.

618 Harrigan, S., Zsoter, E., Alfieri, L., Prudhomme, C., Salamon, P., Wetterhall, F., Barnard, C., Cloke,
619 H., and Pappenberger, F.: GloFAS-ERA5 operational global river discharge reanalysis 1979–
620 present, *Earth System Science Data*, 12, 2043-2060, [https://doi.org/10.5194/essd-12-2043-](https://doi.org/10.5194/essd-12-2043-2020)
621 [2020](https://doi.org/10.5194/essd-12-2043-2020), 2020.

622 Hirpa, F. A., Alfieri, L., Lees, T., Peng, J., Dyer, E., and Dadson, S. J.: Streamflow response to climate
623 change in the Greater Horn of Africa, *Climatic Change*, 156, 341-363,
624 <https://doi.org/10.1007/s10584-019-02547-x>, 2019.

625 Jiang, Y. and Liu, Z.: Evaluations of Remote Sensing-Based Global Evapotranspiration Datasets at
626 Catchment Scale in Mountain Regions, *Remote Sensing*, 13, 5096,
627 <https://doi.org/10.3390/rs13245096>, 2021.

628 Jung, H. C., Getirana, A., Arsenault, K. R., Holmes, T. R. H., and McNally, A.: Uncertainties in
629 Evapotranspiration Estimates over West Africa, *Remote Sensing*, 11, 892,
630 <https://doi.org/10.3390/rs11080892>, 2019.

631 Kabuya, P. M., Hughes, D. A., Tshimanga, R. M., Trigg, M. A., and Bates, P.: Establishing
632 uncertainty ranges of hydrologic indices across climate and physiographic regions of the
633 Congo River Basin, *Journal of Hydrology: Regional Studies*, 30, 100710,
634 <https://doi.org/10.1016/j.ejrh.2020.100710>, 2020.

635 Kamta, F. N., Schilling, J., and Scheffran, J.: Water Resources, Forced Migration and Tensions with
636 Host Communities in the Nigerian Part of the Lake Chad Basin, *Resources*, 10, 27, 2021.

637 Kiang, J. E., Gazoorian, C., McMillan, H., Coxon, G., Le Coz, J., Westerberg, I. K., Belleville, A.,
638 Sevrez, D., Sikorska, A. E., Petersen-Øverleir, A., Reitan, T., Freer, J., Renard, B.,
639 Mansanarez, V., and Mason, R.: A Comparison of Methods for Streamflow Uncertainty
640 Estimation, *Water Resources Research*, 54, 7149-7176,
641 <https://doi.org/10.1029/2018WR022708>, 2018.

642 Koukoulas, M., Nikolopoulos, E. I., Dokou, Z., and Anagnostou, E. N.: Evaluation of global water
643 resources reanalysis products in the upper Blue Nile River Basin, *Journal of*
644 *Hydrometeorology*, 21, 935-952, <https://doi.org/10.1175/JHM-D-19-0233.1>, 2020.

645 Krabbenhoft, C. A., Allen, G. H., Lin, P., Godsey, S. E., Allen, D. C., Burrows, R. M., DelVecchia,
646 A. G., Fritz, K. M., Shanafield, M., Burgin, A. J., Zimmer, M. A., Datry, T., Dodds, W. K.,
647 Jones, C. N., Mims, M. C., Franklin, C., Hammond, J. C., Zipper, S., Ward, A. S., Costigan,
648 K. H., Beck, H. E., and Olden, J. D.: Assessing placement bias of the global river gauge
649 network, *Nature Sustainability*, 2022.

- 650 Krinner, G., Viovy, N., de Noblet-Ducoudré, N., Ogée, J., Polcher, J., Friedlingstein, P., Ciais, P.,
651 Sitch, S., and Prentice, I. C.: A dynamic global vegetation model for studies of the coupled
652 atmosphere-biosphere system, *Global Biogeochemical Cycles*, 19,
653 <https://doi.org/10.1029/2003GB002199>, 2005.
- 654 Laipelt, L., Kayser, R. H. B., Fleischmann, A. S., Ruhoff, A., Bastiaanssen, W., Erickson, T. A., and
655 Melton, F.: Long-term monitoring of evapotranspiration using the SEBAL algorithm and
656 Google Earth Engine cloud computing, *ISPRS Journal of Photogrammetry and Remote
657 Sensing*, 178, 81-96, <https://doi.org/10.1016/j.isprsjprs.2021.05.018>, 2021.
- 658 Lakew, H. B., Moges, S. A., Anagnostou, E. N., Nikolopoulos, E. I., and Asfaw, D. H.: Evaluation
659 of global water resources reanalysis runoff products for local water resources applications:
660 case study-upper Blue Nile basin of Ethiopia, *Water Resources Management*, 34, 2157-2177,
661 <https://doi.org/10.1007/s11269-019-2190-y>, 2020.
- 662 Larbi, I., Hountondji, F. C. C., Dotse, S.-Q., Mama, D., Nyamekye, C., Adeyeri, O. E., Djan'na
663 Koubodana, H., Odoom, P. R. E., and Asare, Y. M.: Local climate change projections and
664 impact on the surface hydrology in the Vea catchment, West Africa, *Hydrology Research*, 52,
665 1200-1215, <https://doi.org/10.2166/nh.2021.096>, 2021.
- 666 Liu, W.: Evaluating remotely sensed monthly evapotranspiration against water balance estimates at
667 basin scale in the Tibetan Plateau, *Hydrology Research*, 49, 1977-1990, 10.2166/nh.2018.008,
668 2018.
- 669 López, P. L., Sultana, T., Kafi, M. A. H., Hossain, M. S., Khan, A. S., and Masud, M. S.: Evaluation
670 of global water resources reanalysis data for estimating flood events in the Brahmaputra River
671 Basin, *Water Resources Management*, 34, 2201-2220, <https://doi.org/10.1007/s11269-020-02546-z>, 2020.
- 672
673 Ma, N., Szilagyi, J., and Zhang, Y.: Calibration-free complementary relationship estimates terrestrial
674 evapotranspiration globally, *Water Resources Research*, 57, e2021WR029691, 2021.
- 675 Martens, B., Miralles, D. G., Lievens, H., Van Der Schalie, R., De Jeu, R. A., Fernández-Prieto, D.,
676 Beck, H. E., Dorigo, W. A., and Verhoest, N. E.: GLEAM v3: Satellite-based land evaporation
677 and root-zone soil moisture, *Geoscientific Model Development*, 10, 1903-1925,
678 <https://doi.org/10.5194/gmd-10-1903-2017>, 2017.
- 679 McNally, A., Arsenault, K., Kumar, S., Shukla, S., Peterson, P., Wang, S., Funk, C., Peters-Lidard,
680 C. D., and Verdin, J. P.: A land data assimilation system for sub-Saharan Africa food and
681 water security applications, *Scientific data*, 4, 1-19, 2017.
- 682 McNamara, I., Baez-Villanueva, O. M., Zomorodian, A., Ayyad, S., Zambrano-Bigiarini, M., Zaroug,
683 M., Mersha, A., Nauditt, A., Mbuliro, M., and Wamala, S.: How well do gridded precipitation
684 and actual evapotranspiration products represent the key water balance components in the
685 Nile Basin?, *Journal of Hydrology: Regional Studies*, 37, 100884,
686 <https://doi.org/10.1016/j.ejrh.2021.100884>, 2021.
- 687 Moriasi, D., G. Arnold, J., W. Van Liew, M., L. Bingner, R., D. Harmel, R., and L. Veith, T.: Model
688 Evaluation Guidelines for Systematic Quantification of Accuracy in Watershed Simulations,
689 *Transactions of the ASABE*, 50, 885-900, <https://doi.org/10.13031/2013.23153>, 2007.
- 690 Mu, Q., Zhao, M., and Running, S. W.: Improvements to a MODIS global terrestrial
691 evapotranspiration algorithm, *Remote sensing of environment*, 115, 1781-1800,
692 <https://doi.org/10.1016/j.rse.2011.02.019>, 2011.
- 693 Mu, Q., Heinsch, F. A., Zhao, M., and Running, S. W.: Development of a global evapotranspiration
694 algorithm based on MODIS and global meteorology data, *Remote sensing of Environment*,
695 111, 519-536, <https://doi.org/10.1016/j.rse.2007.04.015>, 2007.
- 696 Nagabhatla, N., Cassidy-Neumiller, M., Francine, N. N., and Maatta, N.: Water, conflicts and
697 migration and the role of regional diplomacy: Lake Chad, Congo Basin, and the Mbororo
698 pastoralist, *Environmental Science & Policy*, 122, 35-48,
699 <https://doi.org/10.1016/j.envsci.2021.03.019>, 2021.

700 Neal, J., Schumann, G., Bates, P., Buytaert, W., Matgen, P., and Pappenberger, F.: A data assimilation
701 approach to discharge estimation from space, *Hydrological Processes*, 23, 3641-3649,
702 <https://doi.org/10.1002/hyp.7518>, 2009.

703 Nkiaka, E.: Water security assessment in ungauged regions using the water balance and water
704 footprint concepts and satellite observations, *Hydrology Research*,
705 <https://doi.org/10.2166/nh.2022.124>, 2022.

706 Nkiaka, E., Nawaz, N., and Lovett, J.: Using self-organizing maps to infill missing data in hydro-
707 meteorological time series from the Logone catchment, Lake Chad basin, *Environmental*
708 *Monitoring and Assessment*, 188, 1-12, <https://doi.org/10.1007/s10661-016-5385-1>, 2016.

709 Nkiaka, E., Bryant, R. G., Okumah, M., and Gomo, F. F.: Water security in sub-Saharan Africa:
710 Understanding the status of sustainable development goal 6, *WIREs Water*, 8, e1552,
711 <https://doi.org/10.1002/wat2.1552>, 2021.

712 Nkiaka, E., Taylor, A., Dougill, A. J., Antwi-Agyei, P., Adefisan, E. A., Ahiataku, M. A., Baffour-
713 Ata, F., Fournier, N., Indasi, V. S., and Konte, O.: Exploring the need for developing impact-
714 based forecasting in West Africa, *Frontiers in Climate*, 11,
715 <https://doi.org/10.3389/fclim.2020.565500>, 2020.

716 Odusanya, A. E., Mehdi, B., Schürz, C., Oke, A. O., Awokola, O. S., Awomeso, J. A., Adejuwon, J.
717 O., and Schulz, K.: Multi-site calibration and validation of SWAT with satellite-based
718 evapotranspiration in a data-sparse catchment in southwestern Nigeria, *Hydrology and Earth*
719 *System Sciences*, 23, 1113-1144, <https://doi.org/10.5194/hess-23-1113-2019>, 2019.

720 Oussou, F. E., Ndehedehe, C. E., Oloukoi, J., Yalo, N., Boukari, M., and Diaw, A. T.:
721 Characterization of the hydro-geological regime of fractured aquifers in Benin (West-Africa)
722 using multi-satellites and models, *Journal of Hydrology: Regional Studies*, 39, 100987,
723 <https://doi.org/10.1016/j.ejrh.2021.100987>, 2022.

724 Rodell, M., McWilliams, E. B., Famiglietti, J. S., Beaudoin, H. K., and Nigro, J.: Estimating
725 evapotranspiration using an observation based terrestrial water budget, *Hydrological*
726 *Processes*, 25, 4082-4092, <https://doi.org/10.1002/hyp.8369>, 2011.

727 Rodell, M., Houser, P., Jambor, U., Gottschalck, J., Mitchell, K., Meng, C.-J., Arsenault, K.,
728 Cosgrove, B., Radakovich, J., and Bosilovich, M.: The global land data assimilation system,
729 *Bulletin of the American Meteorological society*, 85, 381-394,
730 <https://doi.org/10.1175/BAMS-85-3-381>, 2004.

731 Rodell, M., Beaudoin, H. K., L'Ecuyer, T. S., Olson, W. S., Famiglietti, J. S., Houser, P. R., Adler,
732 R., Bosilovich, M. G., Clayson, C. A., Chambers, D., Clark, E., Fetzer, E. J., Gao, X., Gu, G.,
733 Hilburn, K., Huffman, G. J., Lettenmaier, D. P., Liu, W. T., Robertson, F. R., Schlosser, C.
734 A., Sheffield, J., and Wood, E. F.: The Observed State of the Water Cycle in the Early Twenty-
735 First Century, *Journal of Climate*, 28, 8289-8318, <https://doi.org/10.1175/JCLI-D-14-00555.1>, 2015.

736

737 Rodríguez, E., Sánchez, I., Duque, N., Arboleda, P., Vega, C., Zamora, D., López, P., Kaune, A.,
738 Werner, M., and García, C.: Combined use of local and global hydro meteorological data with
739 hydrological models for water resources management in the Magdalena-Cauca Macro Basin-
740 Colombia, *Water Resources Management*, 34, 2179-2199, 2020.

741 Saha, S., Moorthi, S., Wu, X., Wang, J., Nadiga, S., Tripp, P., Behringer, D., Hou, Y.-T., Chuang,
742 H.-y., and Iredell, M.: The NCEP climate forecast system version 2, *Journal of climate*, 27,
743 2185-2208, <https://doi.org/10.1175/JCLI-D-12-00823.1>, 2014.

744 Satgé, F., Defrance, D., Sultan, B., Bonnet, M.-P., Seyler, F., Rouche, N., Pierron, F., and Paturel, J.-
745 E.: Evaluation of 23 gridded precipitation datasets across West Africa, *Journal of Hydrology*,
746 581, 124412, 2020.

747 Schellekens, J., Dutra, E., Martínez-De La Torre, A., Balsamo, G., Van Dijk, A., Sperna Weiland, F.,
748 Minvielle, M., Calvet, J.-C., Decharme, B., and Eisner, S.: A global water resources ensemble
749 of hydrological models: the earthH2Observe Tier-1 dataset, *Earth System Science Data*, 9, 389-
750 413, 2017.

751 Senay, G. B., Bohms, S., Singh, R. K., Gowda, P. H., Velpuri, N. M., Alemu, H., and Verdin, J. P.:
752 Operational evapotranspiration mapping using remote sensing and weather datasets: A new
753 parameterization for the SSEB approach, *JAWRA Journal of the American Water Resources*
754 *Association*, 49, 577-591, <https://doi.org/10.1111/jawr.12057>, 2013.

755 Sheffield, J., Wood, E. F., Pan, M., Beck, H., Coccia, G., Serrat-Capdevila, A., and Verbist, K.:
756 Satellite remote sensing for water resources management: Potential for supporting sustainable
757 development in data-poor regions, *Water Resources Research*, 54, 9724-9758, 2018.

758 Shen, Z., Yong, B., Gourley, J. J., Qi, W., Lu, D., Liu, J., Ren, L., Hong, Y., and Zhang, J.: Recent
759 global performance of the Climate Hazards group Infrared Precipitation (CHIRP) with
760 Stations (CHIRPS), *Journal of Hydrology*, 591, 125284,
761 <https://doi.org/10.1016/j.jhydrol.2020.125284>, 2020.

762 Sikder, M., David, C. H., Allen, G. H., Qiao, X., Nelson, E. J., and Matin, M. A.: Evaluation of
763 available global runoff datasets through a river model in support of transboundary water
764 management in South and Southeast Asia, *Frontiers in Environmental Science*, 171,
765 <https://doi.org/10.3389/fenvs.2019.00171>, 2019.

766 Slater, L. J., Anderson, B., Buechel, M., Dadson, S., Han, S., Harrigan, S., Kelder, T., Kowal, K.,
767 Lees, T., and Matthews, T.: Nonstationary weather and water extremes: a review of methods
768 for their detection, attribution, and management, *Hydrology and Earth System Sciences*, 25,
769 3897-3935, <https://doi.org/10.5194/hess-25-3897-2021>, 2021.

770 Smith, M. W., Willis, T., Alfieri, L., James, W. H. M., Trigg, M. A., Yamazaki, D., Hardy, A. J.,
771 Bisselink, B., De Roo, A., Macklin, M. G., and Thomas, C. J.: Incorporating hydrology into
772 climate suitability models changes projections of malaria transmission in Africa, *Nature*
773 *Communications*, 11, 4353, <https://doi.org/10.1038/s41467-020-18239-5>, 2020.

774 Tapley, B. D., Watkins, M. M., Flechtner, F., Reigber, C., Bettadpur, S., Rodell, M., Sasgen, I.,
775 Famiglietti, J. S., Landerer, F. W., Chambers, D. P., Reager, J. T., Gardner, A. S., Save, H.,
776 Ivins, E. R., Swenson, S. C., Boening, C., Dahle, C., Wiese, D. N., Dobslaw, H., Tamisiea,
777 M. E., and Velicogna, I.: Contributions of GRACE to understanding climate change, *Nature*
778 *Climate Change*, 9, 358-369, <https://doi.org/10.1038/s41558-019-0456-2>, 2019.

779 Thiemi, V., Bisselink, B., Pappenberger, F., and Thielen, J.: A pan-African medium-range ensemble
780 flood forecast system, *Hydrol. Earth Syst. Sci.*, 19, 3365-3385, [https://doi.org/10.5194/hess-](https://doi.org/10.5194/hess-19-3365-2015)
781 [19-3365-2015](https://doi.org/10.5194/hess-19-3365-2015), 2015.

782 UNDESA: United Nations, Department of Economic and Social Affairs, Population Division Prospects, Volume
783 I: Comprehensive Tables (ST/ESA/SER.A/426), 2019.

784 van Beek, L. P. H., Wada, Y., and Bierkens, M. F. P.: Global monthly water stress: 1. Water balance
785 and water availability, *Water Resources Research*, 47,
786 <https://doi.org/10.1029/2010WR009791>, 2011.

787 Van Der Knijff, J. M., Younis, J., and De Roo, A. P. J.: LISFLOOD: a GIS-based distributed model
788 for river basin scale water balance and flood simulation, *International Journal of Geographical*
789 *Information Science*, 24, 189-212, 10.1080/13658810802549154, 2010.

790 van Dijk, A. I. J. M., Renzullo, L. J., Wada, Y., and Tregoning, P.: A global water cycle reanalysis
791 (2003–2012) merging satellite gravimetry and altimetry observations with a
792 hydrological multi-model ensemble, *Hydrol. Earth Syst. Sci.*, 18, 2955-2973,
793 <https://doi.org/10.5194/hess-18-2955-2014>, 2014.

794 Wada, Y., Wisser, D., and Bierkens, M. F. P.: Global modeling of withdrawal, allocation and
795 consumptive use of surface water and groundwater resources, *Earth Syst. Dynam.*, 5, 15-40,
796 <https://doi.org/10.5194/esd-5-15-2014>, 2014.

797 Weedon, G. P., Balsamo, G., Bellouin, N., Gomes, S., Best, M. J., and Viterbo, P.: The WFDEI
798 meteorological forcing data set: WATCH Forcing Data methodology applied to ERA-Interim
799 reanalysis data, *Water Resources Research*, 50, 7505-7514,
800 <https://doi.org/10.1002/2014WR015638>, 2014.

801 Weerasinghe, I., Bastiaanssen, W., Mul, M., Jia, L., and Van Griensven, A.: Can we trust remote
802 sensing evapotranspiration products over Africa?, *Hydrology and Earth System Sciences*, 24,
803 1565-1586, <https://doi.org/10.5194/hess-24-1565-2020>, 2020.

804 Wiese, D. N., Landerer, F. W., and Watkins, M. M.: Quantifying and reducing leakage errors in the
805 JPL RL05M GRACE mascon solution, *Water Resources Research*, 52, 7490-7502,
806 <https://doi.org/10.1002/2016WR019344>, 2016.

807 Xie, J., Liu, L., Wang, Y., Xu, Y.-P., and Chen, H.: Changes in actual evapotranspiration and its
808 dominant drivers across the Three-River Source Region of China during 1982–2014,
809 *Hydrology Research*, <https://doi.org/10.2166/nh.2022.076>, 2022.

810 Zhang, Y., Kong, D., Gan, R., Chiew, F. H. S., McVicar, T. R., Zhang, Q., and Yang, Y.: Coupled
811 estimation of 500 m and 8-day resolution global evapotranspiration and gross primary
812 production in 2002–2017, *Remote Sensing of Environment*, 222, 165-182,
813 <https://doi.org/10.1016/j.rse.2018.12.031>, 2019.

814 Zhang, Y., Peña-Arancibia, J. L., McVicar, T. R., Chiew, F. H., Vaze, J., Liu, C., Lu, X., Zheng, H.,
815 Wang, Y., and Liu, Y. Y.: Multi-decadal trends in global terrestrial evapotranspiration and its
816 components, *Scientific reports*, 6, 1-12, <https://doi.org/10.1038/srep19124>, 2016.

817